Journal of Alloys and Compounds 509 (2011) 9609–9616

Contents lists available at ScienceDirect

Journal of Alloys and Compounds

journal homepage: www.elsevier.com/locate/jallcom

Effect of ageing on microstructure and mechanical properties of bulk, cryorolled, and room temperature rolled Al 7075 alloy

Sushanta Kumar Panigrahi, R. Jayaganthan*

Department of Metallurgical and Materials Engineering, Indian Institute of Technology Roorkee, Roorkee, Uttarakhand 247667, India

ARTICLE INFO

Article history:
Received 31 March 2011
Received in revised form 10 July 2011
Accepted 11 July 2011
Available online 23 July 2011

Keywords:
Cryorolling
Room temperature rolling
Al 7075 alloy
Ageing
Tensile properties
Ultrafine grained microstructure

ABSTRACT

The effect of ageing on mechanical properties and microstructural characteristics of a precipitation hardenable Al 7075 alloy subjected to rolling at liquid nitrogen temperature and room temperature are has been investigated in the present work employing hardness measurements, tensile test, XRD, DSC, and TEM. The solution-treated bulk Al 7075 alloy was subjected to cryorolling and room temperature rolling to refine grain structures and subsequently ageing treatment to simultaneously improve the strength and ductility. The solution treatment combined with cryorolling up to a true rolling strain of 2.3 followed by low temperature ageing at 100 °C for 45 h has been found to be the optimum processing condition to obtain fine grained microstructure with improved tensile strength (642 MPa) and good tensile ductility (9.5%) in the Al 7075 alloy. The combined effect of suppression of dynamic recovery, partial grain refinement, partial recovery, solid solution strengthening, dislocation hardening, and precipitation hardening are responsible for the significant improvement strength–ductility combination in the cryorolled Al 7075 alloy subjected to peak ageing treatment. The cryorolled and room temperature rolled Al 7075 alloy, upon subjecting to peak ageing treatment, have shown higher strength and ductility in the former than the latter. It is due to presence of high density of nanosized precipitates in the peak aged cryorolled sample.

1. Introduction

The precipitation hardenable Al alloys are extensively used in automobile and aerospace structures and many other high strength structural components due to their high strength to weight ratio (specific strength), excellent mechanical properties, high thermal and electrical conductivity, and superior resistance to oxidation and corrosion [1]. An increased usage of these alloys depends on enhancing their mechanical properties such as strength and toughness further from the values achieved so far in the bulk alloys. It is well known that refining the grain structure to ultrafine regime can enhance the mechanical properties of these bulk Al alloys further [2]. Cryorolling has been identified as one of the potential routes to produce bulk ultrafine grained Al alloys from its bulk alloys at cryogenic temperature [2–16]. The ultrafine grained bulk Al alloy sheets could be exploited for commercial application if its strength and ductility are improved simultaneously. However, it is difficult to achieve simultaneous improvement of strength and ductility of ultrafine grained Al alloys as reported in the literature [17–21]. The low ductility of ultrafine grained materials is due to its inability to accumulate dislocations [20–23].

Recently, a lot of research activities are focused to improve the strength and ductility of severely deformed age hardenable Al alloys [2,24–33]. The effect of post-ECAP low-temperature ageing on the tensile behavior of an Al 10.8 wt pct Ag alloy was studied by Horita et al. [24]. They reported that, the work hardening of the ECAP material was improved by producing nano precipitates in the grain volume due to post-ECAP ageing treatment. Kim et al. [25] investigated the effect of low temperature ageing on strength and ductility of an ECAP-processed Al 2024 alloy and found that the yield strength improved to ~630 MPa while maintaining a reasonable elongation to failure (~15 pct). Zheng et al. [26,27] studied the effect of ageing on the strength of the ECAP processed Al 7050 alloy and identified that the pre-ECAP solid solution treatment combined with the post-ECAP low-temperature ageing process has significantly improved its strength. Kim et al. [28] have studied the influence of ageing on ECAP processed Al 7075 alloy containing Sc (7×51) and reported a significant enhancement of strength properties after subjecting it to proper ageing treatment. The studies reported to date are confined mainly to the ageing effect on ECAP processed Al–Zn–Mg–Cu alloys. Since cryorolling was adopted in the present investigation as a processing route to produce ultrafine grained microstructure, the study of ageing effect on cryorolled Al 7075 alloy is very much essential in order to improve its mechanical properties further. The ageing kinetics of CR Al 7075 alloy samples is not subjected to a detailed study so far in the literature. Although Zhao et al. [2] have proposed a low temperature ageing treatment

* Corresponding author. Tel.: +91 1332 285869; fax: +91 1332 285243.
E-mail address: rjayafmt@iitr.ernet.in (R. Jayaganthan).

0925-8388/$ – see front matter © 2011 Elsevier B.V. All rights reserved.
doi:10.1016/j.jallcom.2011.07.028

to the cryorolled Al 7075 alloy to improve its both strength and ductility, the influence of ageing kinetics on mechanical properties of this alloy has not been studied so far.

Since cryorolling and room temperature rolling are two competitive processes to refine the grain structure, it is important to substantiate the effectiveness of the post processing age hardening behavior of Al 7075 alloy rolled under both temperature. It is also important to compare the age hardening behavior of bulk, solution treated samples with cryorolled samples as well as room temperature rolled samples. Owing to these facts, the present work has been focused: (i) to study the effect of ageing on mechanical properties and microstructure of cryorolled Al 7075 alloy; (ii) to study the effect of ageing on microstructure and mechanical properties of room temperature rolled Al 7075 alloy; (iii) to compare the age hardening behavior of bulk, solution treated Al 7075 alloy samples with that of cryorolled as well as room temperature rolled Al 7075 alloy samples.

2. Experimental

The Al 7075 alloy extruded ingot with the diameter of 250 mm was procured from Hindustan Aeronautics Ltd., Bangalore. The chemical composition of this material is 5.5 Zn, 2.6 Mg, 1.55 Cu, 0.2 Cr, 0.2 Si, 0.15 Mn, 0.3 Fe, and Al balance. The as received material was machined into the dimensions of 12 mm × 30 mm × 40 mm. These machined plates were solution treated (ST) at 490 °C for 6 h and then quenched in water. The ST Al 7075 alloy plates were then cryorolled (CR) and room temperature rolled (RTR) up to a true strain of 2.3. In cryorolling, the Al 7075 alloy plates are rolled at liquid nitrogen temperature until receiving the required strain of 2.3. Prior to each cryorolling pass, the materials are dipped into liquid nitrogen for 20 min and then these samples are rolled again. The diameter of the rolls was 110 mm and the rolling speed was 8 rpm.

These ST plates and CR and RTR sheets were then subjected to artificial ageing at four different temperatures such as 80 °C, 100 °C, 120 °C and 140 °C with the ageing durations up to 100 h to study the influence of age hardening behavior. The microstructural features of the ST, CR and RTR Al 7075 alloy samples before and after ageing at different temperatures were examined in details by transmission electron microscope (TEM) analysis, differential scanning calorimetry (DSC), and X-ray diffraction (XRD). In order to evaluate the strength and ductility of the cryorolled Al 7075 alloy samples subjected to the different ageing treatments, microhardness and tensile tests were conducted. The sample dimensions and sample preparation procedure for TEM, DSC, XRD, hardness test and tensile test are described in detail in our earlier work [13,25].

3. Results

3.1. Mechanical properties

The hardness of the CR and RTR samples has increased from 107 to 190 Hv (nearly 78% increase) and 107 to 180 Hv (nearly 68% increase), respectively, at a rolling strain of 2.3 as shown in Fig. 1. In order to improve the mechanical properties of the ST, CR and RTR samples, the samples were subjected to post-ageing treatment and shown in Fig. 1. The hardness data of the Al 7075 alloy samples (ST, CR and RTR) measured after ageing at 140 °C vs. ageing time up to

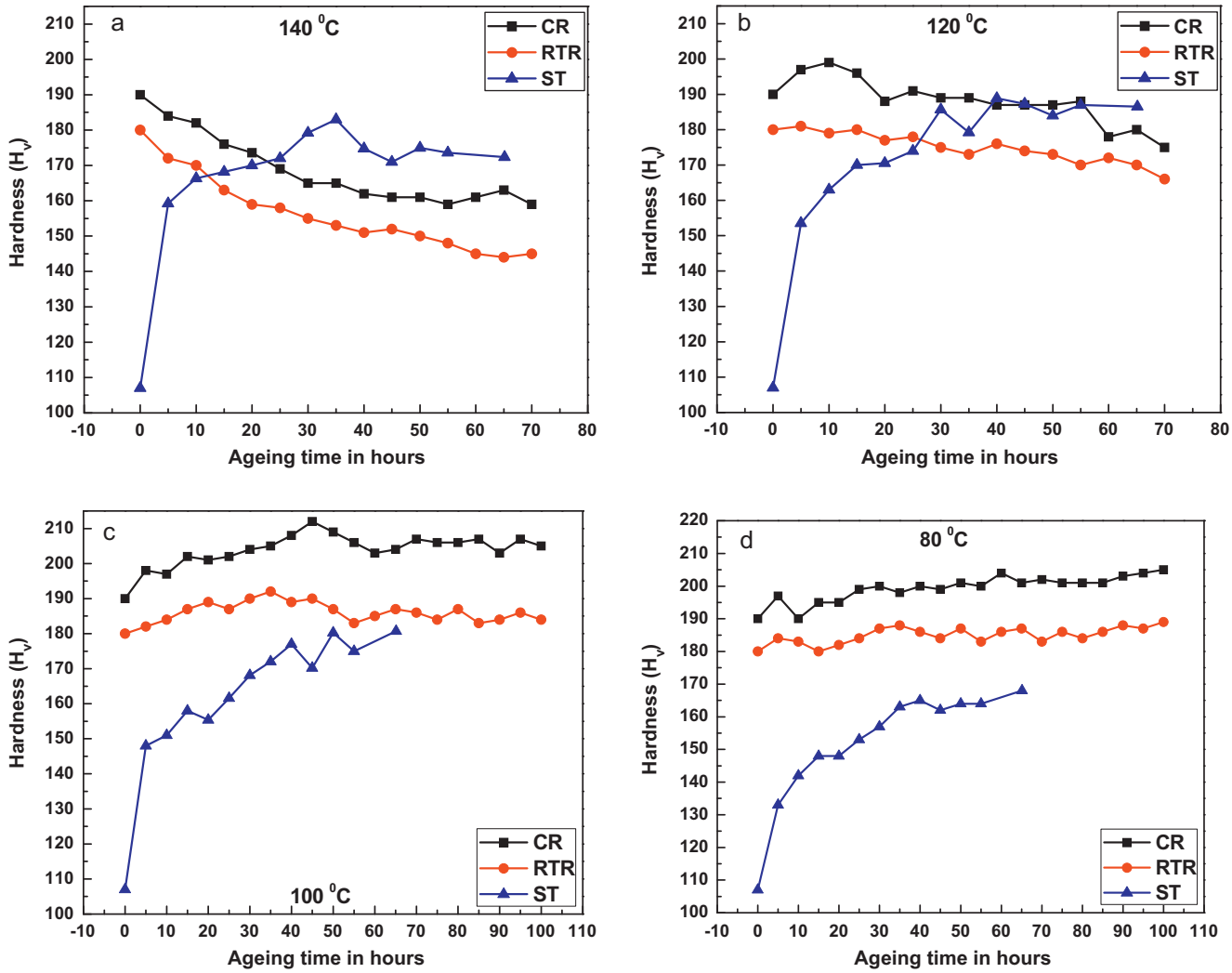

Fig. 1. Vickers hardness of the CR, RTR and bulk (ST) Al 7075 alloy vs. ageing time at (a) 140 °C, (b) 120 °C, (c) 100 °C and (d) 80 °C.

Table 1
The tensile data of Al 7075 alloy at different conditions.

Different conditions	YS (MPa)	UTS (MPa)	UE	TE
ST	155	368	16.6	18.5
ST + PA (T6)	502	572	9.0	11.0
RTR	529	578	4.2	5.2
RTR + PA	577	618	6.0	8.2
CR	545	591	5.0	5.6
CR + PA	607	642	8.2	9.5

70 h is shown in Fig. 1a. There is a significant increase in hardness up to 35 h (71% increase) and then it decreases in case of ST samples. On the other hand, the CR and RTR samples exhibit an opposite trend; hardness decreases with time. It may be because of the recovery effect which might have occurred during a high temperature ageing of the CR and RTR samples with time. The effect of ageing treatment at 120 °C up to 70 h on the ST, CR and RTR samples is shown in Fig. 1b. The hardness of the CR and ST samples is increased from 190 to 199 Hv and 107 to 189 Hv, respectively. However, the hardness decreases with ageing time for RTR samples.

In order to minimize the softening effect, the ST, CR and RTR samples were aged at lower temperatures such as 100 °C and 80 °C. The effect of ageing on hardness value of ST, CR and RTR samples as a function of time at temperatures of 100 °C and 80 °C are shown in Fig. 1c and d, respectively. At an ageing temperature of 100 °C, the hardness of CR samples increases, approximately 12%, after 45 h. For the RTR samples, an increase in hardness is also observed at 35 h, but the hardening effect is less as compared to that of CR samples. A significant increase in hardness (69% increases) is also observed in the ST samples. When the ST, CR and RTR samples are subjected to ageing treatment at 80 °C, the increase in hardness with ageing time is observed in all the three materials. However, the increase in hardness is not saturated up to 100 h for CR and RTR samples and up to 65 h for ST samples.

After optimizing the peak ageing condition of the ST, CR and RTR samples as shown in Fig. 2, the tensile test was carried out for all these samples with the peak ageing condition at 120 °C for 30 h, 100 °C for 45 h and 100 °C for 35 h, respectively. The tensile stress–strain curves (both engineering and true stress–strain curves) of the ST sample, ST sample with peak ageing (PA) treatment, CR sample, CR sample with PA treatment, RTR sample, and RTR sample with PA treatment are shown in Fig. 2 and Table 1. The uniform elongation (as mentioned in Table 1 and marked by the symbol □ on the true stress–strain curves in Fig. 2b) was calculated by using the criterion (Eq. (1)), which governs the onset of localized deformation [2,3],

$$\left(\frac{\partial\sigma}{\partial\varepsilon}\right)_{\dot{\varepsilon}} \tag{1}$$

where σ and ε are true stress and true strain, respectively.

As compared to the ST samples, the YS and UTS of the CR samples have increased from 155 MPa to 545 MPa and 368 MPa to 591 MPa, respectively. Similarly, the YS and UTS have increased from 155 MPa to 529 MPa and 368 MPa to 578 MPa, respectively, in the RTR materials as compared to ST materials. However, the ductility (both uniform elongation (UE) and elongation to failure (FE)) has decreased for both CR as well as RTR samples. The YS and UTS of the CR samples after peak ageing (CR + PA) have increased from 545 to 607 MPa and 591 to 642 MPa, respectively, as compared to the CR materials. Along with the YS and UTS, the ductility of the CR samples after post ageing treatment (ductility: 9.5) has increased about 70% than that of CR samples (ductility: 5.6) as well as RTR samples (ductility: 5.2). When the RTR samples are subjected to PA treatment (RTR + PA), the YS and UTS have increased from 529 to

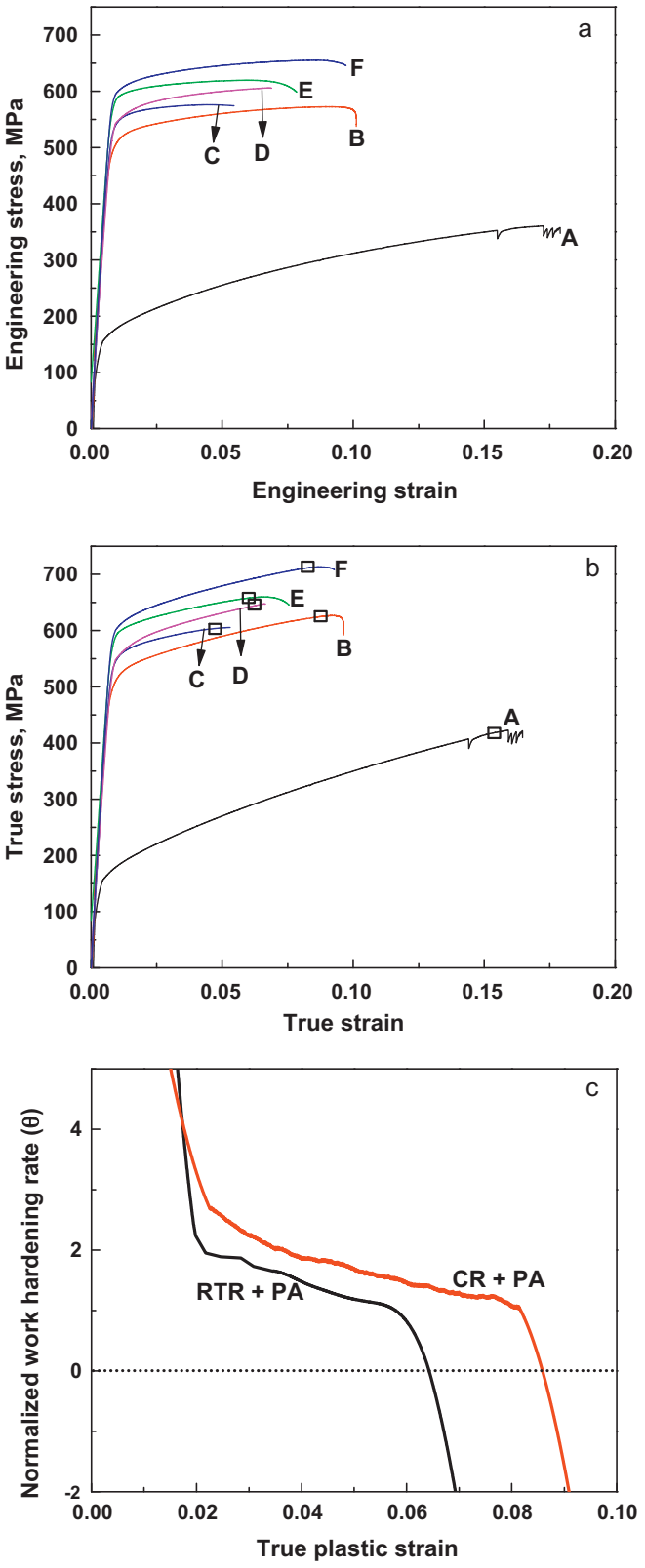

Fig. 2. Tensile stress–strain curves of Al 7075 alloy at various conditions (A) ST, (B) ST + PA, (C) RTR, (D) CR, (E) RTR + PA, and (F) CR + PA; (a) engineering stress–strain curves, (b) true stress–strain curves, and (c) comparison of work hardening rate plots of two types of samples.

577 MPa and 578 to 618 MPa, respectively, as compared to that of RTR samples.

The YS and UTS of the CR + PA samples are higher than that of RTR + PA samples. As compared to RTR + PA samples, the UE and TE of the CR + PA samples are 26% and 14% higher, respectively. In order to investigate the work hardening behavior of the CR + PA and RTR + PA samples, the normalized work-hardening rate, θ ($\theta = (1/\sigma)(\partial\sigma/\partial\varepsilon)$), as a function of true plastic strain is plotted in Fig. 2c. The CR + PA samples show higher work hardening rate than RTR + PA samples. The higher work hardening rate in CR + PA samples (Fig. 2c) as compared to RTR + PA samples is responsible for achieving higher ductility in CR + PA samples.

The observed tensile properties (UTS: 572 MPa, YS: 502 MPa and ELONG: 11) of the ST material after peak ageing treatment (120 °C for 30 h) shown in Fig. 2 and Table 1 correspond to the T6-peak ageing condition for a commercial Al 7075 alloy. As compared to the T6 treatment, the YS, UTS of the CR samples with the PA treatment have increased from 502 MPa to 607 MPa and 572 MPa to 642 MPa, respectively. Where as, in case of RTR sample subjected to PA treatment, a comparatively lower strengthening effect is observed.

3.2. XRD results before and after peak ageing treatment

Fig. 3a shows the XRD results of ST, CR and RTR samples without subjecting to PA treatment. The ST and CR samples show the absence of the $MgZn_2$ precipitates. However, a small intensity peak of $MgZn_2$ is observed in the RTR samples. XRD analysis was also conducted for ST, CR and RTR samples subjected to PA treatments to see the contribution of different precipitates and compounds in enhancing their mechanical properties. Fig. 3b shows the comparative XRD plots of ST, CR, and RTR samples subjected to three optimized peak ageing treatments such as 120 °C for 30 h, 100 °C for 45 h and 100 °C for 35 h, respectively. The XRD results show the formation of fine $MgZn_2$ precipitates in all the three peaks of PA treated samples.

3.3. DSC analysis before and after peak ageing treatment

The DSC curves obtained at heating rates of 40 °C/min for ST, CR and RTR samples before ageing treatment are shown in Fig. 4a. The DSC curves of the ST samples show four exothermic peaks and two endothermic peaks. The four exothermic reaction peaks as numbered in Fig. 4a (A) such as peaks 1, 2, 3 and 4 represent the GP (I) zone, GP (II) zone, formation of η' phase and formation η phase, respectively [34]. The endothermic peaks such as 5 and 6 represent the dissolution of metastable η' precipitates and η phases, respectively. It is seen that all the reaction peaks corresponding to the formation and dissolution of different precipitate reactions of CR and RTR samples are shifting to left when compared to that of its ST samples. As compared to RTR samples, all the reaction peaks corresponding the formation and dissolution of different precipitate reactions of CR samples are shifting to left. The formation of all the precipitate reactions as mentioned above is observed in ST samples. In case of RTR samples, the peaks associated with the formation of GP (I) zone and GP (II) zone are not observed. A new endothermic peak is also observed in the range of 175–225 °C in the RTR samples, which may be due to the dissolution of GP zones. In the CR samples, all the above mentioned reaction peaks are observed except GP (I) zone. Fig. 4b shows the DSC plots of ST, RTR and CR samples after subjecting them to the PA treatments. In all the three peak aged samples, the peaks associated with the formation of GP (I) zone, GP (II) zone and η' phase have disappeared and only the formation of stable peak for η phase is observed.

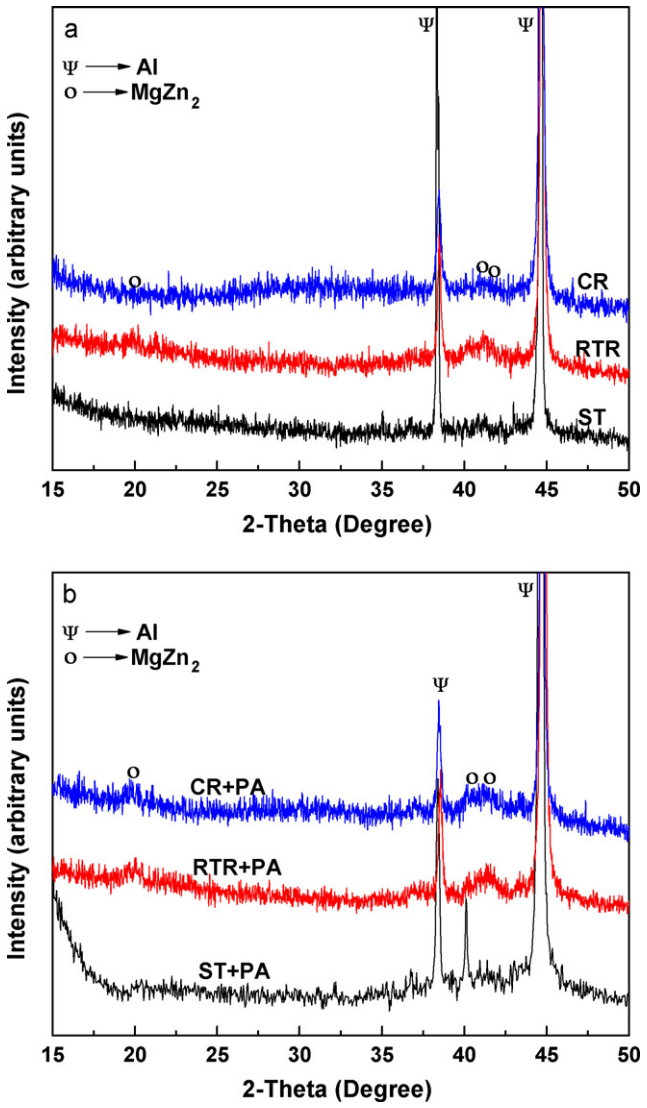

Fig. 3. XRD analysis of ST, RTR and CR Al 7075 alloy samples with and without PA treatment: (a) without PA treatment, (b) with PA treatment.

3.4. TEM analysis before and after peak ageing treatment

The CR and RTR samples after subjecting to PA treatment (100 °C for 45 h) were investigated in TEM to analyze the precipitation morphology and shown in Fig. 5. The presence of plate shaped and spherical shaped precipitates is found in the microstructure. The TEM study of the CR and RTR samples before and after PA treatment was conducted to investigate the evolution of microstructure such as changes in dislocation content, subgrain morphology, formation of recrystallized grains and shown in Figs. 6 and 7. The heavily strained sub grains and elongated grains are evident in both conditions (CR and RTR samples) from the Fig. 6. A heavily deformed microstructure was observed in the CR samples. However, a much better-defined subgrains is observed in RTR samples. The presence of dislocation as observed in CR samples is rarely seen in RTR samples. When the CR and RTR samples are subjected to PA treatments, there is not much change in microstructures of both materials (Fig. 7). The microstructure of both materials shows a slight reduction of dislocation density and slight relaxation of cell boundaries into subgrain walls. Most of the nonequilibrium grain boundaries are still not recovered in both PA samples and dislocations are still observed in the grain interiors.

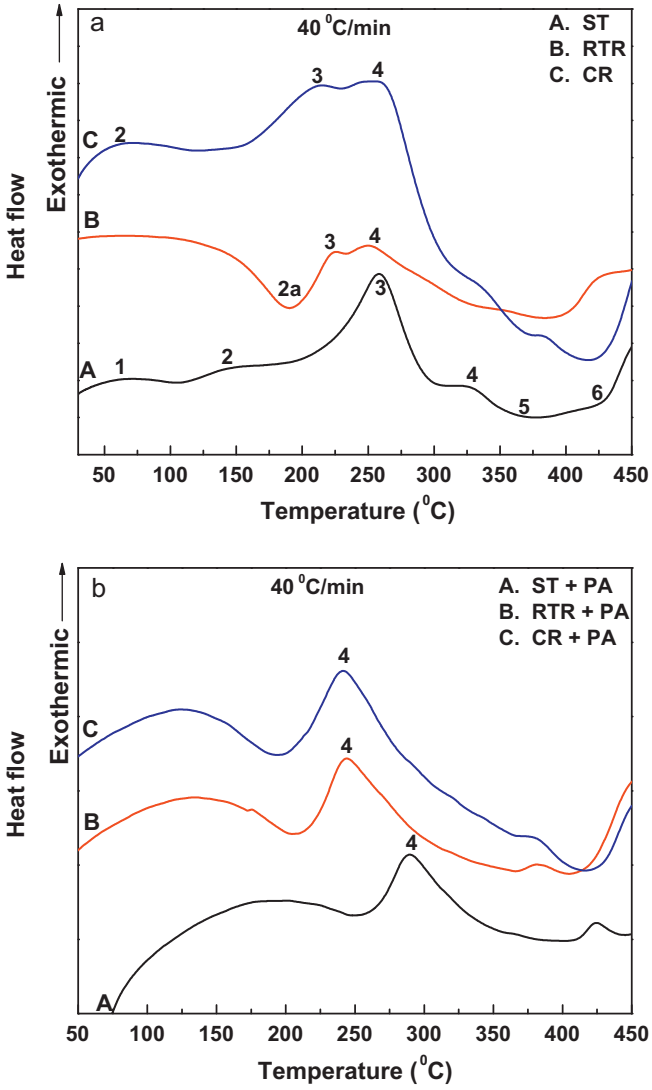

Fig. 4. DSC plots of ST, RTR and CR Al 7075 alloy samples with and without PA treatment: (a) without PA treatment, (b) with PA treatment.

Based on the TEM results of CR and RTR samples subjected to PA treatment, it is evident that the PA temperature and time is not enough to recrystallize the microstructure completely. Therefore, the microstructure may be stable for low temperature applications, but not stable for high temperature applications.

4. Discussion

The influence of ageing treatment on mechanical properties of CR 7075 Al alloy was studied in detail by hardness testing and tensile testing. A comparatively higher initial strength and hardness of the CR samples than that of RTR samples before ageing treatment is due to the effective suppression of dynamic recovery and accumulation of higher amount of dislocation density due to cryogenic rolling.

When the ST samples are subjected to PA treatment, a significant increase in hardness (77% increases), yield strength (224% increase) and tensile strength (56% increase) is observed. In CR samples with PA treatment, the increase in hardness, yield strength (YS) and tensile strength (UTS) are observed to be 12%, 11.4% and 9%, respectively. However, a comparatively less improvement in strengthening properties (YS (9.1%), UTS (7%) increase) is observed for RTR samples subjected to PA treatment. The possible reasons for

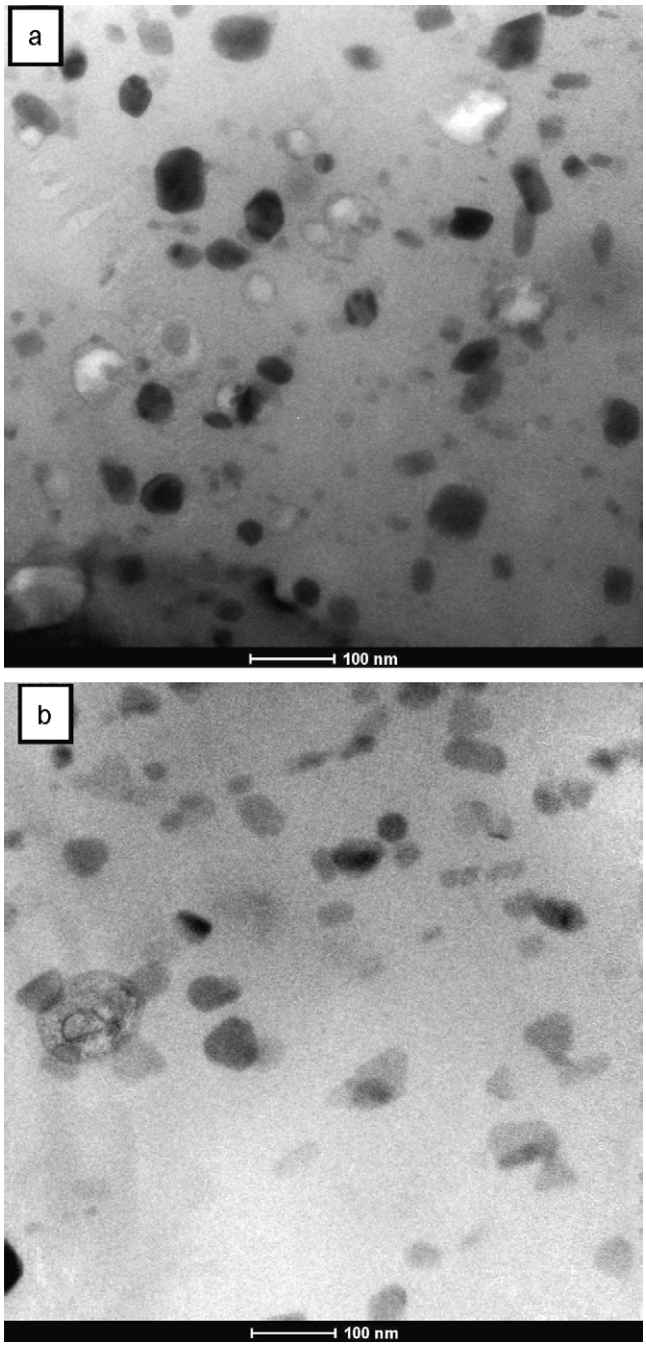

Fig. 5. TEM images for precipitate distribution of CR and RTR samples of Al 7075 alloy at a strain of 2.3 after peak ageing treatment: (a) CR sample, (b) RTR sample.

large increase in strength and hardness of ST samples as compared to both CR and RTR samples are as follows. During solutionizing and quenching of the ST samples, the solute atoms are completely dissolved in the solid solution and the internal strain from the samples is also completely relieved as well as the dislocations are completely annihilated. So, during ageing treatment of the quenched samples, the applied temperature (120 °C) acts as a driving force for transformation of metastable solute to stable precipitates. At the PA state, maximum amount of coherent/semi coherent precipitates of mostly η' phase are present and these precipitate particles acts as obstacles for dislocation movement, resulting in maximum strength of ST samples. Hence, the effect of precipitation hardening plays the dominant role for its large enhancement of strength and hardness. Since the CR and RTR samples are deformed up to a

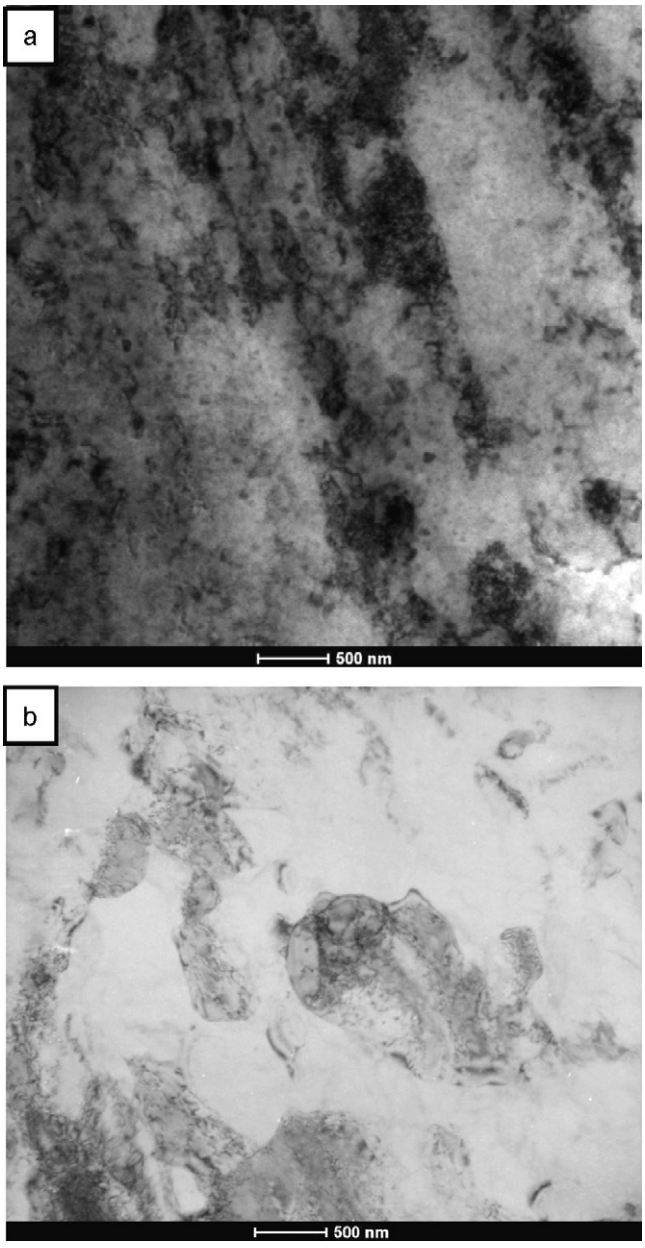

Fig. 6. TEM images of CR and RTR Al 7075 alloy samples at a strain of 2.3: (a) CR sample, (b) RTR sample.

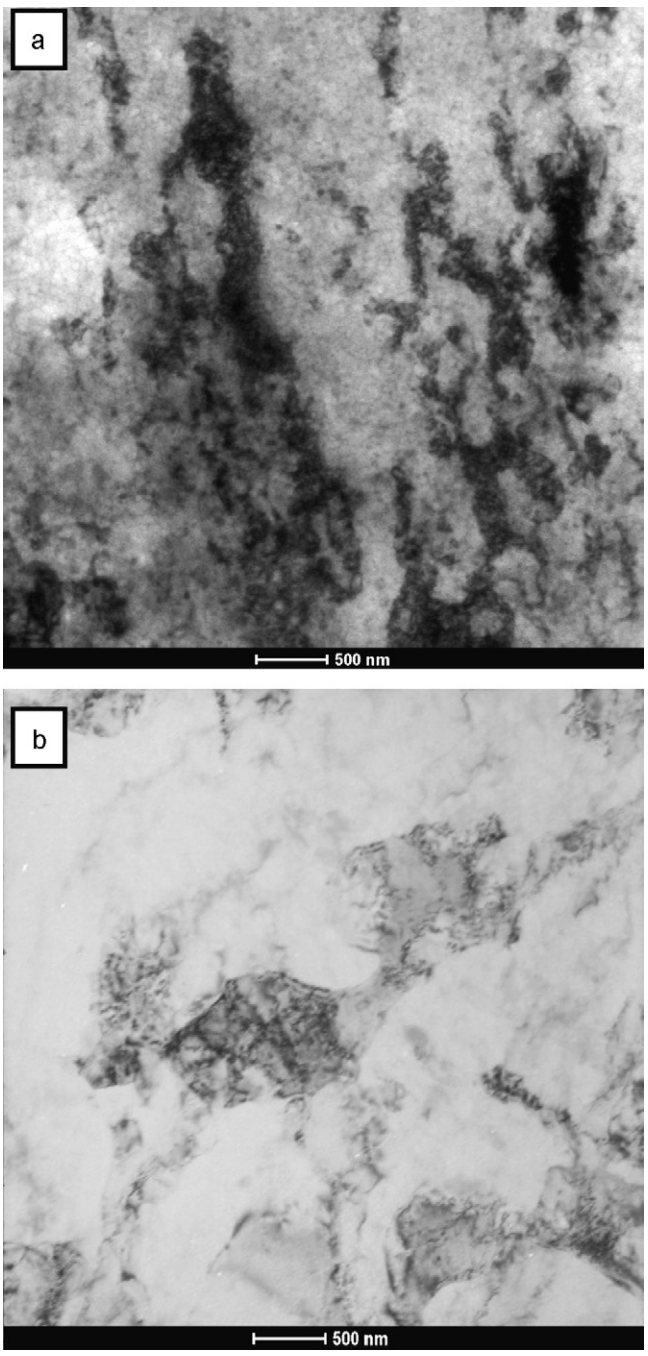

Fig. 7. TEM images of CR and RTR Al 7075 alloy samples at a strain of 2.3 after subjecting to PA treatment: (a) CR sample, (b) RTR sample.

strain of 2.3, a heavy amount of dislocations and strain energy are stored in the samples. When these heavily deformed samples are subjected to PA treatment, the effect of recovery and precipitation hardening occurs simultaneously. During high temperature ageing treatments (140 °C and 120 °C), the recovery effect is dominating the precipitation hardening effect, causing the decrease in hardness. Similarly, during low temperature ageing treatments (100 °C and 80 °C), the precipitation hardening is dominating over recovery, due to which increase in hardness is observed. Since both recovery and hardening act simultaneously in the CR and RTR samples, the resultant effect of increase in strength and hardness is less than that of ST samples after PA treatment.

After subjecting PA treatment to the CR and RTR samples, it is observed that the CR samples exhibit better strength and hardness than that of RTR samples. The XRD results (Fig. 3a) show the presence of a small intensity peak of $MgZn_2$ phase in the RTR samples before ageing treatment. However, it is not observed in case of CR samples prior to ageing treatment. The DSC results (Fig. 4a) of the CR samples show the appearance of all the reaction peaks such as, the formation of GP (II) zone, formation of η' phase and formation η phase, respectively. However, the peaks corresponding to the formation of GP zones are not observed in the RTR samples before the ageing treatment and the observed endothermic peak is due to dissolution of GP zones. From XRD results and DSC analysis, it is confirmed that the precipitation of GP zones has occurred during room temperature rolling. The frictional heat is generated between the rollers and sample during room temperature rolling, due to which the sample are heated up to 50–70 °C. It is known that GP zone is one of the strengthening phases of Al 7075 alloy. When the RTR samples are subjected to PA treatment, the precipitation hardening associated with GP zone formation will not occur;

causing lesser overall hardening effect on the sample. However, for the CR samples, the metastable solute does not get sufficient thermal energy to precipitate the solutes from solid solution during cryorolling. Therefore, after cryorolling, all the metastable solutes are still retained in the solid solution. When the CR samples are peak aged, a significant strengthening effect is observed due to all the strengthening phases such as GP zones and η′ phase precipitates.

The DSC results in Fig. 4b show the absence of GP zones and η′ phase precipitates in the ST, RTR and CR samples after PA treatment. Also, in all the three PA treated samples, the peak associated with the formation of the stable η phase is observed. It clearly indicates that the increase in strength in all the three PA treated samples is due to the intermediate precipitates. Based on the DSC results of CR samples subjected PA treatment, it is confirmed that the plate shaped particles and spherical shaped particles as observed from the TEM microstructure (Fig. 6) are η′ phase precipitate particles and GP zones. When the sample containing these spherical GP zones and plate shaped η′ phase precipitate particles are subjected to tensile testing, these coherent nanosized precipitates acts as the obstacles for the dislocation movement due to tensile straining. Hence, a higher strength is required to either overcome or cut through these precipitates, which results in a significant increase in both yield strength and tensile strength of the CR samples subjected to PA treatment.

4.1. Factors affecting strength

The significant high strength of ST, RTR and CR Al 7075 alloy after peak ageing treatment may be attributed to (i) solid solution strengthening, (ii) grain refinement, (iii) dislocation strengthening, and (iv) precipitation hardening. Solid solution strengthening of Al 7075 alloy depends upon the concentration of solute in the solid solution. When the Al 7075 alloy samples are solutionized and quenched, the solute atoms such as Zn, Mg, Cu, Fe and Mn are dissolved in the matrix in the substitutional sites. So, strength of the parent material increases due to differences in the size, modulus or valency of the solute and parent atoms. Since the concentration of solutes in Al 7075 alloy is relatively more as compared to other precipitation hardenable Al alloys, it may give a significant strengthening effect to the ST, RTR and CR samples after PA treatment.

The strengthening due to grain refinement is mainly described by the Hall–Petch equation [35,36]. The TEM microstructure of CR and RTR samples after PA treatment indicates that most of the grains in both samples are still elongated and not recrystallized. Also, only a partial fraction of grains is recrystallized in both the CR and RTR samples. Hence, the grain refinement is not the main contributor for the strength enhancement of the ST, RTR and CR samples after PA treatment.

The TEM microstructures of CR and RTR samples after PA treatment revealed high dislocation density, suggesting that the dislocation strengthening has significant contribution to the strength enhancement in both samples. Since a comparatively higher dislocation density is observed in the CR samples as compared to the RTR samples, the dislocation strengthening contribution is higher in the former than the latter after PA treatment. However, this strengthening contribution is not observed in case of ST samples.

The precipitation strengthening results from ability of the precipitates to impede dislocation motion. Since the precipitates density of the CR samples is higher than that of the RTR samples, its strengthening effect is more in CR samples than the latter. It is evident that the precipitation strengthening is one of the main contributors for the strength enhancement of the ST, RTR and CR samples after PA treatment.

The factors influencing the strength of the ST, CR and RTR samples subjected to PA treatment can also be explained by using Taylor relationship given below (Eq. (1)), which is based on the dislocation theory [37–39]:

$$\sigma_y = \sigma_0 + \alpha M^{\mathrm{T}} G b \rho^{1/2} + 0.85 M^{\mathrm{T}} \frac{Gb \ln(x/b)}{2\pi(l-x)} \quad (2)$$

where σ_0, α, G, b, M^{T}, ρ, x and l are the friction stress, a constant, shear modulus, Burgers vector, Taylor factor, dislocation density, average size of precipitates, and intermetallic spacing, respectively. The strengthening effect due to all the three terms is well manifested in CR and RTR samples. However, the strength contribution due to the second term is not manifested in the ST samples.

As per Eq. (1), the yield strength of the materials is directly proportional to the dislocation density. The dislocation density in the CR samples is enhanced due to the combined effect of interaction between dislocations, grain boundaries (Hall–Petch effect), and the presence of solutes in solid solution. On the other hand, few of the dislocation densities are annihilated during rolling at room temperature of the RTR samples, which result in lesser strengthening effect due to second term of Eq. (1). So, the strengthening effect due to the first two terms of CR samples is higher than the RTR samples.

The third term from Eq. (1) contributes the precipitation hardening behavior of all ST, CR and RTR samples. During room temperature rolling, GP zones are formed. When these samples are subjected to PA treatment, transformation of GP zones to η′ phase precipitate occurs. In the CR samples subjected to PA treatment, the presence of GP zones and η′ phase precipitates is observed. As the size of the precipitates (GP zones and η′ phase precipitates) in the CR samples after PA treatment is smaller than that of RTR samples subjected to PA treatment (η′ phase precipitates), the volume fraction of nanosized precipitates in CR samples after PA treatment is more. Due to this, the interparticle spacing (l) between the precipitates in the CR samples is less as compared to that of RTR samples. If the average precipitate size (x) is assumed to be same for both CR and RTR samples, the lower interparticle spacing of CR sample would contribute to the improved strength due to third term of Eq. (1) which is higher than that of RTR samples. As per Eq. (1), the strength contribution due to all the terms of CR samples subjected to the PA treatment are higher than that of RTR and ST samples with their PA treated states, realizing the enhanced strength of CR samples.

4.2. Factors affecting ductility

Along with the improvement of strength, a significant improvement of ductility is also observed in the CR and RTR samples after PA treatments. The CR and RTR samples after PA treatment, shows an increase in ductility of 70% and 58%, respectively, than that of CR and RTR samples without ageing treatment. The existing reported strategies for achieving improved ductility in nanostructured materials are either due to the distribution of bimodal grain size [40,41], or by sacrificing their strength [42] or by restricting their service conditions to low temperatures and high strain rates [43,44]. However, the TEM microstructures (Fig. 7) in the present investigation do not show any results, matching with the existing literature.

The effective enhancement of ductility of both CR and RTR samples after PA treatment may be due to the following reasons: (i) due to annihilation of dislocations during the PA treatment, it leaves a scope for dislocation accumulation before saturation, during tensile testing, which contributes a significant enhancement of ductility and (ii) due to the presence of nanosized precipitates in the peak aged samples, the dislocations are accumulated in the surrounding of the nanosized precipitates during tensile straining. Since the density of the precipitates is more, it accumulates higher amount of dislocations causing tensile straining for a prolonged period of

time, contributing to the enhanced ductility, the similar observations were reported by Zhao et al. [2] and Cheng et al. [3]. Zhao et al. [2] investigated the influence of duplex ageing (50 °C for 5 h and then at 80 °C for 9 h) on mechanical properties of cryorolled Al 7075 alloy. The improvement in ductility observed in the present work is in tandem with their work.

The ductility of the CR samples after peak ageing treatment is higher than that of RTR samples. Since the density of the nanosized precipitates in CR samples after PA treatment is more than that of the RTR samples after PA treatment, it provides more effective sites to trap and accumulate the dislocations surrounding to the precipitates. Therefore, during tensile straining of the CR samples subjected to PA treatment, the sample elongates substantially (higher ductility) prior to failure due to its higher dislocation accumulation capacity enabled by nanosized precipitates. Hence, cryorolling followed by ageing is an effective method to improve both the strength and ductility simultaneously. This strategy may be implemented to many of the precipitation hardenable alloys. Also, the dynamic precipitation during room temperature rolling should be avoided; because the effect of ductility gets less pronounced when the RTR samples are further aged.

5. Conclusions

The effect of ageing on mechanical properties and microstructure of ST, CR and RTR Al 7075 alloy has been investigated in the present work. The following conclusions are made:

- At higher ageing temperature of 140 °C, the hardness of the CR and RTR samples decreases with ageing time. It may be because of the recovery effect, which might have occurred during a high temperature ageing of the CR and RTR materials with time.
- The higher rate of increase in strength and hardness of peak aged ST samples is observed than that of CR and RTR samples. It is because of the precipitation hardening effect is manifested in the ST samples. However, the CR and RTR samples receive a combined effect such as softening effect due to recovery and hardening effect due to precipitation hardening.
- Cryorolling of Al 7075 alloy with a true rolling strain of 2.3 followed by low temperature ageing at 100 °C for 45 h resulted in grain refinement with improved mechanical properties (YS of 607 MPa, UTS of 642 MPa and tensile ductility of 9.5%) due to the combined effect of suppression of dynamic recovery, partial grain refinement, partial recovery, solid solution strengthening, dislocation hardening, and precipitation hardening.
- As compared to the peak aged (T6) treated Al 7075 alloy samples, the CR and RTR samples after peak ageing treatment shows a significant increase in YS and UTS.
- The TEM microstructures of CR and RTR samples subjected to PA treatment clearly indicate that the microstructure is not completely recrystallized.

References

[1] T. Burg, A. Crosky, Aeronautical Materials, University of New South Wales, 2001, pp. 1–42.
[2] Y.H. Zhao, X.Z. Liao, S. Cheng, E. Ma, Y.T. Zhu, Adv. Mater. 18 (2006) 2280–2283.
[3] S. Cheng, Y.H. Zhao, Y.T. Zhu, E. Ma, Acta Mater. 55 (2007) 5822–5832.
[4] T. Shanmugasundaram, B.S. Murty, V.S. Sarma, Scripta Mater. 54 (2006) 2013–2017.
[5] V.S. Sarma, J. Wang, W.W. Jian, A. Kauffmann, H. Conrad, J. Freudenberger, Y.T. Zhu, Mater. Sci. Eng. A 527 (2010) 7624–7630.
[6] V.S. Sarma, W.W. Jian, H. Conrad, Y.T. Zhu, J. Mater. Sci. 45 (2010) 4846–4850.
[7] T. Konkova, S. Mironov, A. Korznikov, S.L. Semiatin, Acta Mater. 58 (2010) 5862–5873.
[8] Y.B. Chun, S.H. Ahn, D.H. Shin, S.K. Hwang, Mater. Sci. Eng. A 508 (2009) 253–258.
[9] S.K. Panigrahi, R. Jayaganthan, Mater. Des. 32 (2011) 2172–2180.
[10] S.K. Panigrahi, R. Jayaganthan, V. Chawla, Mater. Sci. Eng. A 492 (2008) 300–305.
[11] S.K. Panigrahi, R. Jayaganthan, J. Mater. Sci. 45 (2010) 5624–5636.
[12] S.K. Panigrahi, R. Jayaganthan, Mater. Des. 32 (2011) 3150–3160.
[13] S.K. Panigrahi, R. Jayaganthan, Metall. Mater. Trans. A 41 (2010) 2675–2690.
[14] S.K. Panigrahi, R. Jayaganthan, V. Pancholi, M. Gupta, Mater. Chem. Phys. 122 (2010) 188–193.
[15] H. Miura, T. Sakai, S. Maruokaa, J.J. Jonas, Philos. Mag. Lett. 90 (2010) 93–101.
[16] D.K. Yang, P.D. Hodgson, C.E. Wen, Scripta Mater. 63 (2010) 941–944.
[17] Y.H. Zhao, J.F. Bingert, X.Z. Liao, B.Z. Cui, K. Han, A.V. Sergueeva, A.K. Mukherjee, R.Z. Valiev, T.G. Langdon, Y.T. Zhu, Adv. Mater. 18 (2006) 2949–2953.
[18] C.C. Koch, Scripta Mater. 49 (2003) 657–662.
[19] Y. Zhao, Y. Zhu, E.J. Lavernia, Adv. Eng. Mater. 12 (2010) 769–778.
[20] D. Jia, Y.M. Wang, K.T. Ramesh, E. Ma, Y.T. Zhu, R.Z. Valiev, Appl. Phys. Lett. 79 (2001) 611–613.
[21] Y.T. Zhu, X.Z. Liao, Nat. Mater. 3 (2004) 235–240.
[22] H.V. Swygenhoven, J.R. Weertman, Scripta Mater. 49 (2003) 625–627.
[23] Z. Budrovic, H.V. Swygenhoven, P.M. Derlet, S.V. Petegem, B. Schmitt, Science 304 (2004) 273–276.
[24] Z. Horita, T. Fujinami, T.G. Langdon, Mater. Sci. Eng. A 318 (2001) 34–40.
[25] W.J. Kim, C.S. Chung, D.S. Ma, S.I. Hong, H.K. Kim, Scripta Mater. 49 (2003) 333–337.
[26] L.J. Zheng, C.Q. Chen, T.T. Zhou, P.Y. Liu, M.G. Zeng, Mater. Charact. 49 (2003) 455–461.
[27] L.J. Zheng, H.X. Li, M.F. Hashmi, C.Q. Chen, Y. Zhang, M.G. Zeng, J. Mater. Process. Technol. 171 (2006) 100–107.
[28] W.J. Kim, J.K. Kim, H.K. Kim, J.W. Park, Y.H. Jeong, J. Alloys Compd. 450 (2008) 222–228.
[29] S.K. Panigrahi, R. Jayaganthan, V. Pancholi, Mater. Des. 30 (2009) 1894–1901.
[30] Y.H. Zhao, X.Z. Liao, Z. Jin, R.Z. Valiev, Y.T. Zhu, Acta Mater. 52 (2004) 4589–4599.
[31] Y.H. Zhao, X.Z. Liao, Y.T. Zhu, R.Z. Valiev, J. Mater. Res. 20 (2005) 288–291.
[32] M. Rajamuthamilselvan, S. Ramanathan, J. Alloys Compd. 509 (2011) 948–952.
[33] M.R. Roshan, S.A. Jenabali Jahromi, R. Ebrahimi, J. Alloys Compd. 509 (2011) 7833–7839.
[34] R. Jayaganthan, S.K. Panigrahi, Mater. Sci. Forum 584 (2008) 911–916.
[35] E.O. Hall, Proc. Phys. Soc. Lond. B 64 (1951) 747–753.
[36] N.J. Petch, J. Iron Steel Inst. 174 (1953) 25.
[37] U.F. Kocks, Philos. Mag. 13 (1996) 541–566.
[38] J. Gubicza, I. Schiller, N.Q. Chinh, J. Illy, Z. Horita, T.G. Langdon, Mater. Sci. Eng. A 460 (2007) 77–85.
[39] S.K. Panigrahi, R. Jayaganthan, Mater. Sci. Eng. A 528 (2011) 3147–3160.
[40] M. Wang, F. Chen, Zhou, E. Ma, Nature 419 (2002) 912–915.
[41] Y. Zhao, T. Topping, J.F. Bingert, J.J. Thornton, A.M. Dangelewicz, Y. Li, W. Liu, E.J. Lavernia, Adv. Mater. 20 (2008) 3028–3033.
[42] B.Q. Han, Z. Iee, D. Witkin, S. Nutt, E.J. Lavernial, Metall. Mater. Trans. A 36 (2005) 957–965.
[43] Y.M. Wang, E. Ma, Acta Mater. 52 (2004) 1699–1709.
[44] S. Cheng, Y. Zhao, Y. Guo, Y. Li, Q. Wei, X.L. Wang, Y. Ren, E.J. Lavernia, Adv. Mater. 21 (2009) 5001–5004.